

# In-situ Polymerization of Olefins on Nanoparticles or Fibers by Metallocene Catalysts

W. Kaminsky · A. Funck · C. Klinke

Published online: 4 April 2008  
© Springer Science+Business Media, LLC 2008

**Abstract** This paper shows the capability and advantage of the in-situ polymerization of olefins as a technique for the preparation of nanocomposites. The nanocomposites base on high molecular weight and highly isotactic polypropylenes and oxidized multi-walled carbon nanotubes (HMWiPP/MWCNT). Since a good interfacial adhesion between the matrix and the filler is crucial for the successful preparation of nanocomposites the polymerizations were performed with MAO anchored covalently to the surface of the nanotubes. Thus, a heterogeneous co-catalyst is formed and the polymerization starts directly on the tube surface. The resulting nanocomposites contain 0.9–25 wt% multi-walled carbon nanotubes and polypropylene with a molecular weight of about  $1.4 \times 10^6$  g/mol. They were investigated with respect to their properties, like crystallization and melting temperature, as well as half-time of crystallization which decreases very strong in dependence on a rising filler content. The morphology analysis shows a homogeneous CNT distribution, a good separation of the individual particles, a very good interfacial adhesion and that every nanotube is covered by a thin polymer layer.

**Keywords** Olefin polymerization · Metallocene catalysts

## 1 Introduction

The in-situ polymerization of polyolefins in presence of nanoparticles or fibers is one of the most efficient and versatile ways to synthesize nanocomposites. Metallocene/methylaluminoxane (MAO) catalysts allow the tailoring of the polymer microstructure, tacticity, and stereoregularity, by the utilization of a metallocene with a suitable ligand structure [1, 2]. PP with an isotactic, syndiotactic, or atactic configuration can be obtained by using  $C_2$ -,  $C_{2v}$ -, or  $C_5$ -symmetric zirconocenes [3, 4]. These catalysts are also excellent tools in the production of copolymers. Metallocene/MAO catalysts are highly active for the production of precisely designed polyolefins and engineering plastics [5–9] and also permit the control of the molecular masses.

The most common techniques to prepare nanocomposites are via melt-compounding or solution blending. In the first case molten polymer and the nanofillers are mixed intensively under the exposure of shear forces. Different kinds of mixing devices, such as a twin-screw extruder, are available for this task. It is important, that the shear forces exerted by the mixer are sufficient to tear the individual particles apart. Especially in the case of carbon nanotubes (CNT), this can be a serious problem because they have a high tendency to agglomerate due to a very high surface energy [10]. Highly viscous melts of polymers are also inadequate for this method, because the mixing is hindered, and the high shear forces can lead to a partial degradation of the polymer itself. A good dispersion of CNT in polyolefin matrices can only be achieved by simple melt-compounding at low filler contents [11] and low molecular masses and an accordingly low viscosity of its melt.

If a nanocomposite is prepared via solution blending, the filler is mixed with a polymer in solution. In addition to mechanical mixing, ultrasound can be used to separate the

W. Kaminsky (✉) · A. Funck  
University of Hamburg, Institute of Technical  
and Macromolecular Chemistry, Bundesstr. 45,  
20146 Hamburg, Germany  
e-mail: kaminsky@chemie.uni-hamburg.de

C. Klinke  
University of Hamburg, Institute of Physical Chemistry,  
Grindelallee 117, 20146 Hamburg, Germany

filler particles. When the dispersion is satisfactory, the solvent is evaporated to yield the filled polymer. This method is suitable for systems that consist of a polymer which is soluble in common solvents [12] and in which also the nanofiller can be dispersed well. Highly tactic polypropylene especially with high molecular masses is poorly soluble in most low boiling organic solvents, which makes this method problematic for the preparation of PP/CNT based nanocomposites, too.

In both cases the forces, necessary to separate the CNT agglomerates into individual particles, are applied during the compounding process, while in in-situ polymerization they can be applied before.

The in-situ polymerization provides the possibility of a previous CNT separation during a “pre-treatment” in a low viscosity medium like toluene at a comparatively low energy input (e.g., by ultrasound). The matrix is synthesized afterwards in the presence of the (already separated) nanotubes. The resulting nanocomposites are generally indicated by a good separation, homogenous distribution, and a good wetting with polymer [10, 13–15]. Theoretically it should be possible to produce a nanocomposite with any molecular weight at any filler content desired. But there are some preparative problems which occur when high molecular weight polypropylene (HMWPP) is synthesized.

At high molecular weights ( $M_w > 1.0 \times 10^6$  g/mol) there presumably is a strong gelation effect of the growing polymer chains inside the reactor. High tactic PP with high  $M_w$  tend to jell and accumulates as macroscopically strings, which usually entwine themselves around the stirrer axis. If this happens in the presence of nanotubes, the CNT stick to the swollen polymer strings, which in turn lead to an inadequate CNT distribution.

To avoid these problems we used a modified pre-treatment, based on our previous works [15]. The pre-treatment is an advancement of the Polymerization-Filling Technique (PFT), which initially investigated in Ziegler-Natta polymerization in the late 1970s by Howard et al. [16, 17] and Enikolopian et al. [18]. Nowadays there are several derivatives of the PFT in context with micro- and nanocomposites and metallocene catalysts in use and the method is no longer limited to acidic filler types, but also with basic and other, e.g., metallic [19] or graphite like surfaces [20, 21].

In our workgroup we immobilized MAO by establishing a covalent bonding between MAO and hydroxyl- and carboxyl-functionalized filler surfaces, such as silica balls (monosphers<sup>®</sup>) [22–24] or oxidized CNT, though impregnating the tubes for 24 h with MAO at rt. Purified and oxidized nanotubes (ox. MWCNT) are bearing functional groups such as hydroxyl or carboxyl on their surfaces. These groups can react with MAO by the formation of

covalent oxygen aluminum bond, without deactivating effects for the catalysts. The MAO is now anchored, but still able to form a catalytically active complex with the metallocene [15].

Solved MAO was removed by a filtration and washing procedure, so that only heterogeneous, bonded co-catalyst remained. Anchored MAO and metallocene generate the active complex and so the polymerization takes place near by the filler surface. This leads to a polymer growth directly on the nanoparticle and results in excellent filler coverage with polymer and promotes the separation of the individual particles during the polymerization. Furthermore, the hydrophobic character of some filler materials such as CNT supports the drawing on the fiber.

## 2 Experimental Part

### 2.1 Materials

All reactions and preparations of the compounds were carried out by standard Schlenk, vacuum, and glove box techniques. Argon (purity > 99.996%) was purchased from Linde and was purified further by Oxisorb of Messer-Griesheim. Toluene was supplied from Merck, dried over potassium hydroxide, and purified by passing through columns filled with molecular sieve (4 Å) and BASF-Catalyst R3-11. Propylene was obtained from Gerling, Holz & Co. Handels GmbH (purity > 95%) and purified by using the same type of columns like for the purification of toluene. Methylaluminumoxane was purchased from Crompton as a 10% solution in toluene. After it was filtered over a D4 fritted glass filter, toluene and trimethylaluminum were removed under reduced pressure. The MAO was used as a 100 mg/mL freshly prepared solution in dry toluene. Triisobutylaluminum (TIBA) was obtained from Aldrich and used as a 1 mol/L solution in toluene. The metallocene catalyst [*rac*-dimethylsilylbis(2-methyl-4-(1-naphyl)indenyl)zirconium dichloride] (**1**) was purchased from Boulder Scientific. The concentration of the solution was 5 mmol/L.

The oxidized multi-walled CNT used were thin straight and coiled (2–20 walls, average outer diameter: 15 nm, length: up to 50 μm) and supplied from Nanocyl S. A. (Sambreville, Belgium).

### 2.2 Pretreatment and Polymerization

All polymerizations were carried out in a 1 L glass autoclave (Büchi) that had been evacuated at 90 °C for 1 h and then flushed several times with argon. The reactor was cooled to 30 °C polymerization temperature, charged with 200 ml toluene and 2.0 ml of TIBA solution was added as scavenger. Then the solution was saturated with propene at

2.0 bar, the pressure was kept constant by using a massflow controller (Brooks Instruments, 5850TR series). The polymerization was started by injection of the metallocene/MAO/ox.MWCNT suspension.

The dry MWCNT were sonicated in a toluene suspension using a Sonoplus homogenizer (HD 2200) equipped with a KE 76 sonotrode. The amplitude was 20 W and the sonication time 60 min. After that 2.0 mL of MAO solution (equivalent to 200 mg of MAO) were added and the suspension was stirred for 24 h. After that the suspension was filtrated over a D4 fritted glass filter and three times washed with hot toluene. The impregnated MWCNT were roughly suspended and then ultrasonic separated again (ampl.: 20 W,  $T = 60$  min). For pre-activation 0.5 mL of the zirconocene solution (**1**) was added and the suspension was introduced into the reactor, after it was stirred for approx. 30 min.

The polymerizations were quenched by addition of 5 mL ethanol. All polymers were stirred with a quench solution consisting of water, ethanol, and hydrochloric acid over night. The solid was filtered off, washed with water and ethanol, and dried under vacuum at 60 °C.

By these method isotactic HWMPP/ox.MWCNT nanocomposites with 0.9–5 wt% filler content were obtained.

### 2.3 Analytical Techniques

Melting temperatures,  $T_m$ , were determined by differential scanning calorimetry (DSC) with a DSC 821e (Mettler-Toledo) from the second heating cycle at a heating rate of 20 K/min. Crystallization temperatures,  $T_c$ , were determined by DSC from the cooling curve (cooling rate 10 K/min) after complete melting at 200 °C for 5 min. All crystallinities were calculated from the melting peak of the second heat on the basis of a crystallization enthalpy of 207 J/g for 100% crystalline isotactic polypropylene [25]. The half-time of crystallization ( $\tau_{0.5}$ ) was determined by isothermal DSC experiments. The samples were quenched to the desired isothermal crystallization temperature (cooling rate 40 K/min) after they were entirely molten at 200 °C for 5 min. Electron microscopy was performed on a Leo 1530 FE-REM (SEM) and on a JEOL JEM-1011 (TEM). For studies on morphology composite cryofractures were used. Gel permeation chromatography was carried out with a Waters GPC 2000 Alliance system equipped with a refractive index detector, viscosimetric detector, and a set of three columns, Styragel type. The particle size for each column was 10  $\mu\text{m}$ , and the pore sizes were 10<sup>3</sup> Å (HT3), 10<sup>4</sup> Å (HT4), and 10<sup>6</sup> Å (HT6). 1,2,4-Trichlorobenzene was used as solvent. The analyses were performed at 140 °C and 1.0 mL/min. The molar weights were also determined by viscosimetry at 408 K using a

Ubbelohde viscometer (capillary 0a,  $K = 0.005 \text{ mm}^2/\text{s}^2$ ) as a 1 mg/ml solution in 50 ml decahydronaphthalin.

### 3 Results and Discussion

The molecular weight of the pure HMWPP was  $M_w = 1,400,000 \text{ g/mol}$  for a metallocene catalyst with a typical polydispersity of two.

The polymer matrix of the composites discussed here had a molecular weight in the range of  $M_w = 1,200,000$ – $1,700,000 \text{ g/mol}$ .  $M_w$  is randomly distributed within this range and no dependence on the filler content could be found. The wide scattering was probably a result of remaining CNT during the viscometric and GPC analyses. The polypropene also showed for catalyst **1** characteristic percentage of isotactic pentads of  $97 \pm 2\%$  [26, 27]. The supported MAO is sterically hindered and, due to the removal of solved MAO, the Al:Zr ratio is not optimal. Still the polymerization activity was determined to an average quantity of  $5,000 \text{ kg}_{\text{Pol}}/(\text{mol}_{\text{Zr}}/\text{h} \times \text{mol}_{\text{Mon}}/\text{l})$ . It was independent of the filler content.

To reinforce high and ultra high molecular mass polypropene with nanotubes through in-situ polymerization a CNT pre-treatment that avoids the uncontrolled gelation of the polymer inside the reactor is necessary. This task was accomplished by linking the co-catalyst covalently to the nanotube surfaces. Purified, oxidized, cap, or sidewall modified nanotubes are bearing functional groups such as hydroxyl or carboxyl on their surfaces. These groups can react with MAO by the formation of covalent oxygen aluminum bonds. This esterification led to immobilized MAO, which can be considered as a heterogeneous co-catalyst then. The anchored methylaluminumoxan is still able to form the catalytically active complex with the zirconocene (**1**) [15]. To prevent the PP from forming a bothering gel, the growing polymer strings must entwine themselves around the nanotubes. Therefore, the polymerization must take place directly and only on the CNT surfaces. To force the catalyst (**1**) to form the active complex only with the inhibited MAO, immobilized on the CNT, no dissolved MAO must be left in the reactor. Consequently unreacted and dissolved co-catalyst was removed by a filtration and washing procedure.

The resulting nanocomposites were in powder form. In Fig. 1, it can be seen that this is not self-evident. As said before especially high molecular weight iPP becomes insoluble during the polymerization process and tends to accumulate itself as a block around the stirrer. The obtained polymer normally must be cut of the stirrer in one piece (Fig. 1a) and had a fibrous surface structure after drying. If the polymerization was performed in the presence of CNT, but without the pre-reaction discussed above

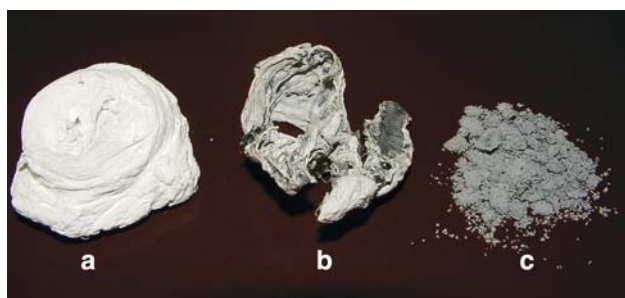


**Fig. 1** (a) Pristine isotactic polypropene,  $M_w = 1,400,000$  g/mol; (b) polymerization was performed with dissolved MAO: no homogenous CNT distribution, nanotubes are accumulated on the PP surface, no composite; (c) polymerization was performed with anchored MAO: CNT are homogenously incorporated into the polymer matrix

the outcome of this is shown in Fig. 1b. Immediately after the HMWPP was beginning to form a gel, the nanotubes stuck on its swollen surface. After a short while the former black suspension got clear and all the nanotubes glue on the PP in one layer. Afterwards only pure PP was synthesized. Thus, the material shown in Fig. 1b was no composite. The only way to obtain a HMWPP/CNT nanocomposite was to polymerize with 100% heterogeneous MAO, accomplishable with our pre-treatment of the CNT (Fig. 1c).

#### 4 Properties of Nanocomposites

The morphology of the HMWPP/CNT nanocomposites was investigated by using scanning electron microscopy (SEM), while transmission electron microscopy (TEM) was used to prove the coating ability of the pre-treatment discussed here and the encapsulation of individual tubes.

As expected the polymer grew directly on the tube surface, which led to a very good coverage and wetting of individual CNT with a thin PP layer. The encapsulation was almost complete and nearly every tube was effected (Fig. 2). It is also obvious that almost every nanotube is coated with an about 10 nm in-situ grown polypropylene film and that there is a good drawing on the tubes. Even the small agglomerate on the lower left side was permeated with polymer and seemed to be widening by the growth of the polymer chains. Figure 3 shows a detailed TEM micrograph of a funnel-shape opened MWCNT. The nanotube consists of 20 walls and is layered by an 8 nm thick in-situ grown PP film. The opened cap is encapsulated too.

The morphology of nanocomposites prepared by in-situ polymerization is, in comparison to melt compounding produced ones, generally indicated by a good CNT separation, homogenous distribution in the matrix, and a good

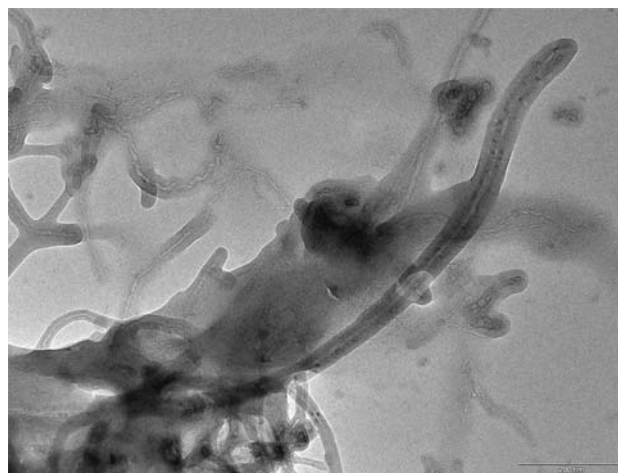


**Fig. 2** TEM micrograph of an HMWPP/MWCNT nanocomposite containing 14 wt% nanotubes. Nearly every nanotube is encapsulated with an about 10 nm in-situ grown polypropylene film

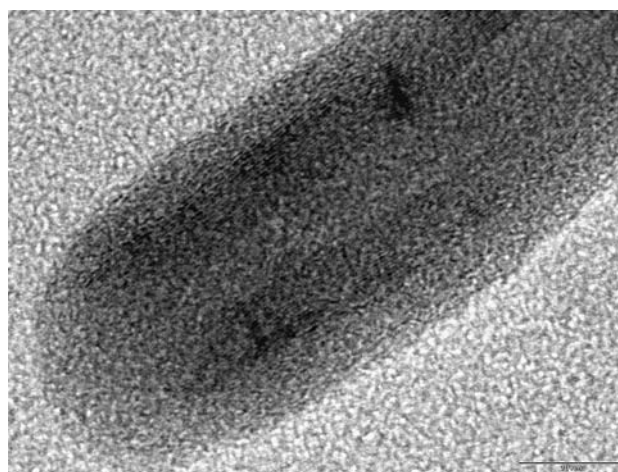


**Fig. 3** Detailed TEM micrograph of an opened MWCNT, covered by a 8 nm thick polymer layer

polymer wetting, which in turn indicates a tight adhesion. Especially the pre-treatment discussed here led to an encapsulating of the tubes with a homogeneous HMWPP layer. SEM micrographs taken from cryofractures of different HMWPP/MWCNT nanocomposites showed no pull-out effect (Figs. 4–7).

A 50,000 fold magnification of such a fracture is shown in Fig. 4, the corresponding composite contained 1.6 wt% MWCNT. It can be seen, that the nanotubes are not aggregated in bundles, but as individual tubes, which indicated a good filler dispersion in this region.

The composite shown in Fig. 5 had a filler content of about 14 wt% and was taken from the powdery form (material, used for TEM micrographics). It consists of a loose network of polymer layered nanotubes, which are partially conglomerated by PP but still mostly separated

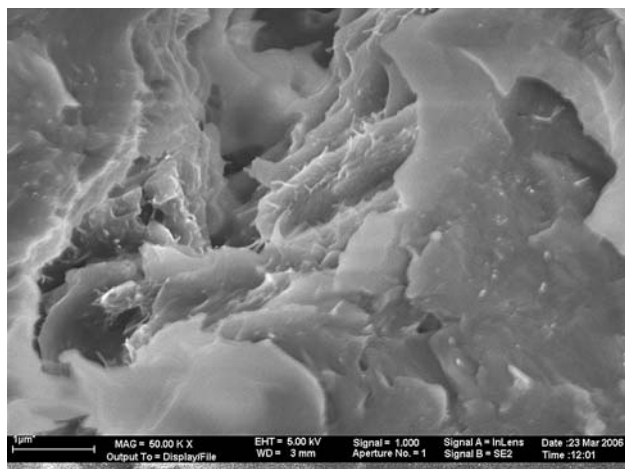


**Fig. 4** SEM micrograph (cryofracture, magnification 50,000 times) of an HMWiPP/MWCNT nanocomposite containing 1.6 wt% nanotubes. A good separation, homogenous distribution, and a good wetting of the nanotubes with HMWiPP was achieved

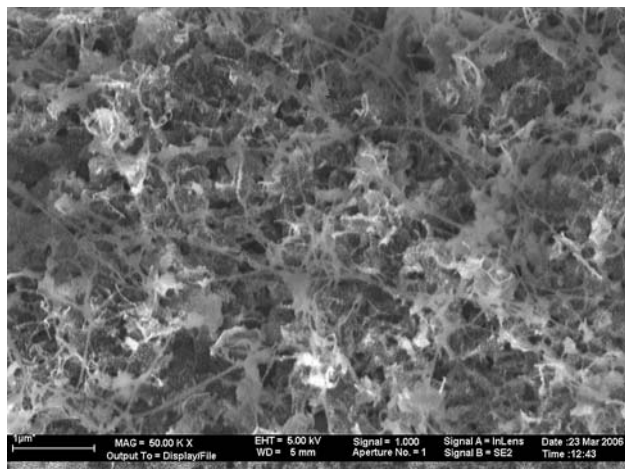


**Fig. 5** SEM micrograph (powder, magnification 50,000 times) of an HMWiPP/MWCNT nanocomposite containing 14 wt% nanotubes. A loose network of polymer layered nanotubes, which are partially conglomerated by PP can be seen

from each other. However, no high-density agglomerates of CNT could be found.

As said before a homogeneous distribution and a good interfacial adhesion are crucial for the successful preparation of nanocomposites. The main challenge in this context is to avoid the slipping of the polymer off the nanotubes (pull-out) under mechanical stress. Figure 6 shows the fracture surface of a HMWPP/CNT with 3.7 wt% filler content. Detailed pictures (Fig. 7) of the plastic stretched area show that there is evidence for the existence of a good load transfer between the matrix and the MWCNT. Even after the rupture process the individual nanotube shown is well wetted with polymer. The neat tube is only visible at

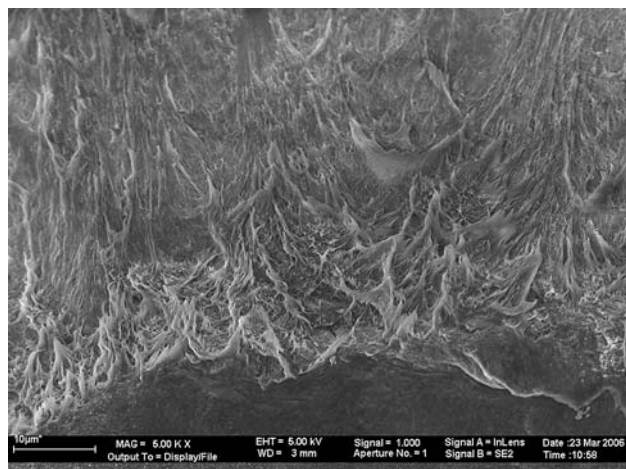


**Fig. 6** SEM micrograph (cryofracture, magnification 5,000 times) of a fracture surface of a HMWiPP/MWCNT nanocomposite with 3.7 wt% filler content

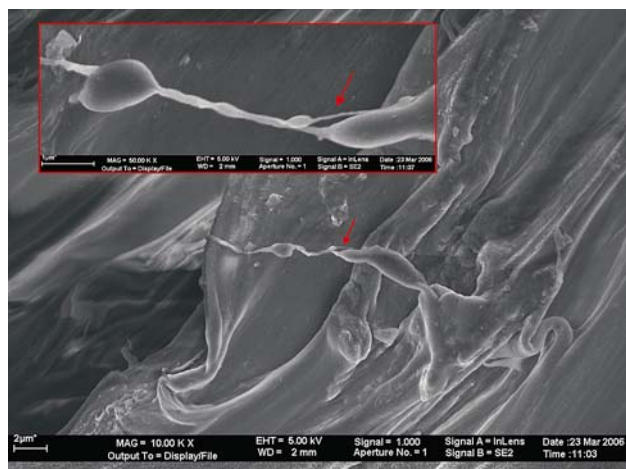


**Fig. 7** SEM micrograph (cryofracture, magnification 10,000 times) of an individual nanotubes, which is well wetted with polymer even after the rupture process. The neat tube is only visible at the position marked. This indicates a good load transfer between the matrix and the MWCNT

the position marked; the rest of the CNT is still covered with PP, which means that the matrix did not slip off the nanotube, but was ripped of. Thus, a maximum amount of the tensile force must be transferred to the nanotube.

The differently loaded nanocomposites were examined according to their crystallization behavior, which plays an important role during the processing of polymeric materials. It is known that CNT act as nucleating agents [28–30], therefore improvements on the crystallization behavior were expected.

Important parameters for the characterization of the crystallization behavior are the crystallization temperature ( $T_c$ ), the melting temperature ( $T_m$ ), and the half-time of crystallization ( $\tau_{0.5}$ ).

$T_m$  was not influenced by the presence of nanotubes or their amount. The average melting temperature was  $160 \pm 1$  °C. Also, the crystallinity was not effected by the CNT and lay in the range of  $45 \pm 4\%$ . In contrary to  $T_m$  the effect on the crystallization temperature was more emphasized. Pure high molecular mass iPP had a  $T_c$  of about 118 °C. The addition of only 0.9 wt% MWCNT led to an increase in crystallization temperature by 5 K. At higher filler contents the crystallization temperature raised rapidly by up to 7 or 8 K above the one of pure iPP leveling at a MWCNT content of about 3 wt% (Fig. 8).

The half-time of crystallization is the length of time needed for 50% of the crystallizable material to solidify from the melt. It depended on the (isothermal) crystallization temperature and on the amount of filler incorporated. At the temperatures shown pristine HMWPP did not crystallize or it took too long to provide reliable results. On the other hand, the crystallization of the obtained nanocomposites was too fast in the range of temperature where the pure iPP gave adequate results. At temperatures above 137 °C composites with CNT contents lower than 2 wt% also did not or needed to long to crystallize.

The half-time of crystallization was significantly reduced by low amounts of nanotubes at all temperatures plotted (Fig. 9). The lower the isothermal  $\tau_{0.5}$  temperature was, the faster the crystallization proceeded. At 135 °C, for instance,  $\tau_{0.5}$  was 4.5 min for a HMWPP/MWCNT composite with 0.9 wt% filler content. The same material required 6.3 min at 137 °C and did not crystallize at 139 °C. When 2.2 wt% were incorporated,  $\tau_{0.5}$  was reduced to only 2.4 min (at 135 °C) and 4.1 min (at 137 °C). This nanocomposite did crystallize at higher temperatures;  $\tau_{0.5}$  was 7.1 min at 139 °C and 8.1 min at 140 °C. When the percentage of MWCNT was raised to more than 3 wt% no significant reduction of  $\tau_{0.5}$  was obtained anymore. This value seems to be the upper limit of the crystallization speed. In contrast to PE-based

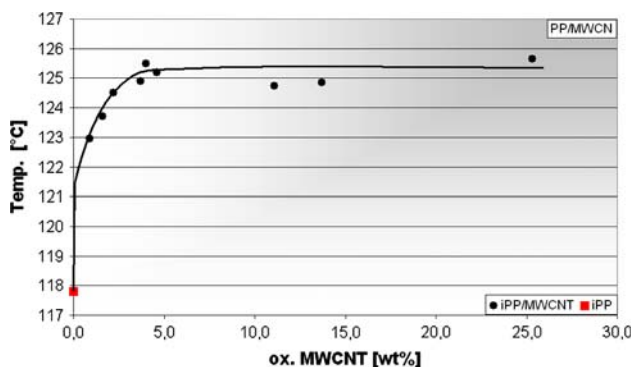


**Fig. 8** Crystallization temperatures of pure iPP and the nanocomposites in dependence on the MWCNT content

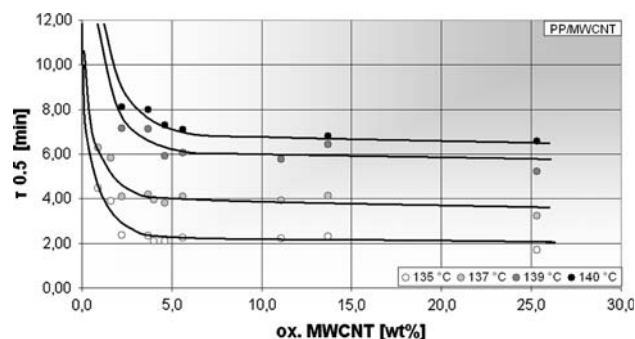


**Fig. 9** Half-time of crystallization of HMWiPP/MWCNT nanocomposites in dependence on the filler content at different isothermal crystallization temperatures

nanocomposites no minimum of the half-time of crystallization was found [31 in preparation]. The half-time of crystallization of CNT nanocomposites was found to decrease in all cited references with regard to the pure polymers [13, 15, 24, 28–30, 32, 33].

## 5 Conclusion

The in-situ polymerization combined with the pre-treatment discussed here offers a way to prepare CNT containing nanocomposites even with a high molecular weight polyolefin matrix. This makes the in-situ polymerization to one of the most efficient and versatile methods to synthesize nanocomposites.

Generally a very good separation, homogenous distribution, and an excellent wetting of the nanotubes with HMWiPP could be achieved. The polymerization took place directly on the CNT surface, which in turn led to an encapsulation of the nanotubes with an about 10 nm thick polymer film.

The crystallization temperature was raised up to 7 or 8 K above the one of pure iPP at a MWCNT content of 3 wt% or higher. The half-time of crystallization was reduced significantly by addition of CNT.

## References

1. Brintzinger HH, Fischer D, Mülhaupt R, Rieger B, Waymouth R (1995) *Angew Chem* 107:1255–1283
2. Kaminsky W (2004) *J Polym Sci Part A Polym Chem* 42: 3911–3921
3. Ewen JA, Jones RL, Razavi A, Ferrara JD (1988) *J Am Chem Soc* 110:6255–6256
4. Resconi L, Cavallo L, Fait A, Piemontesi F (2000) *Chem Rev* 100:1253–1345
5. Kaminsky W (2001) *Adv Catal* 46:89–159
6. Coates GW (2000) *Chem Rev* 100:1223–1252
7. Scheirs J, Kaminsky W (2000) *Metallocene-based polyolefins vols I and II*. Wiley, Chichester
8. Razavi A, Thewalt U (2006) *Coord Chem Rev* 250:155–169

9. Matsui S, Fujita T (2001) *Catal Today* 66:63–73
10. Bonduel D, Mainil M, Alexandre M, Monteverde F, Dubois P (2005) *Chem Commun* 6:781–783
11. Alexandre M, Pluta M, Dubois P, Jérôme R (2001) *Macromol Chem Phys* 202:2239–2246
12. Andrews R, Jaques D, Qian D, Rantell T (2002) *Acc Chem Res* 35:1998–1017
13. Wiemann K, Kaminsky W, Gojny FH, Schulte K (2005) *Macromol Chem Phys* 206:1472–1478
14. Dong X, Wang L, Jiang G, Sun T, Zhao Z, Yu H, Chen T (2006) *J Appl Polym Sci* 101:1291–1294
15. Funck A, Kaminsky W (2007) *Compost Sci Technol* 67(5): 906–915
16. US 4097477 (1978) du Pont de Nemours, E. I. & Co., inv.: J. E. G. Howard, *Chem Abstr* 1978, 89:164489e
17. US 4104243 (1978) du Pont de Nemours, E. I. & Co., inv.: Howard J. E. G., *Chem Abstr* 1979, 90:39708v
18. USSR 763379 (1979) Institute of Chemical Physics, Academy of Science USSR, invs.: Kostandov LA, Enikolopov NS, Dyachkovskii FS, Novokshonova LA, Gavrilov YA, Kudinova OI, Maklakova TA, Akopyan LA, Brikenstein KA 1981, *Chem Abstr* 94:4588m
19. Kaminsky W, Zielonka H (1993) *Polym Adv Technol* 4:415–422
20. Alexandre M, Martin E, Dubois P, Marti MG, Jérôme R (2001) *Chem Mater* 13:236–237
21. Alexandre M, Martin E, Dubois P, Gracia-Marti M, Jerome R (2000) *Macromol Rapid Commun* 21:931
22. Kaminsky W, Wiemann K (2003) *Mirai Zairyo* 3(11):6–12
23. Kaminsky W, Wiemann K (2006) *Comp Interfaces* 13(4–6): 365–375
24. Kaminsky W, Funck A, Wiemann K (2006) *Macromol Symp* 239:1–6
25. Wang ZG, Wang X-H, Hsiao BS, Philips RA, Medellin-Rodriguez FJ, Srinivas S, Wang H, Han CC (2001) *J Polym Sci B* 39:2982–2995
26. Resconi L et al (2000) *Chem Rev* 100:1253–1345
27. Spaleck W, Küber F, Winter A, Rohrmann J, Bachmann B, Antberg M, Dolle V, Paulus E (1994) *Organometallics* 13:954
28. Valentini L, Biagiotti J, Kenny JM, López Manchado MA (2003) *J Appl Polym Sci* 89:2657–2663
29. Wang B, Sun G, Liu J, He X, Li J (2006) *J Appl Polym Sci* 100:3794–3800
30. Assouline EL, Barber AH, Cooper CA, Klein E, Wachtel E, Wagner HD (2003) *J Polym Sci B* 41:520–527
31. Kaminsky W, Funck A (2007) *Macromol Symp* (in preparation)
32. Grady BP, Pompeo F, Shambaugh RL, Resansco DE (2002) *J Phys Chem B* 106:5852–5858
33. Valentini L, Biagiotti J, López-Manchado MA, Santucci S, Kenny JM (2004) *Polym Eng Sci* 44(2):303–311